Vibrational Spectroscopy 58 (2012) 119–124

Contents lists available at SciVerse ScienceDirect

Vibrational Spectroscopy

journal homepage: www.elsevier.com/locate/vibspec

Characterization of surface decorations in Prehispanic archaeological ceramics by Raman spectroscopy, FTIR, XRD and XRF

Silvia A. Centeno[a,*], Veronica I. Williams[b], Nicole C. Little[c], Robert J. Speakman[c]

[a] The Metropolitan Museum of Art, Department of Scientific Research, 1000 Fifth Avenue, New York, NY 10028, USA
[b] Universidad Nacional de Buenos Aires, Facultad Filosofía y Letras, Instituto de Arqueología, 25 de mayo 217, Piso 3, Ciudad Autónoma de Buenos Aires 1002, Argentina
[c] Smithsonian Institution, Museum Conservation Institute, Museum Support Center, 4210 Silver Hill Road, Suitland, MD 20746, USA

ARTICLE INFO

Article history:
Received 2 August 2011
Received in revised form 4 November 2011
Accepted 7 November 2011
Available online 16 November 2011

Keywords:
Raman spectroscopy
XRD
Prehispanic ceramics
Iron manganese spinel
Jacobsite

ABSTRACT

Non-invasive Raman microspectroscopy, FTIR, μXRD and XRF were used to identify the materials present in the black, red, and white surface decorations in selected pottery wares from two Prehispanic archaeological sites in Northwestern (NW) Argentina (AD 900–1530). The iron manganese spinel jacobsite, $MnFe_2O_4$, was found to be the main component of two of the fired black decorations analyzed, while hematite and amorphous silicates were found to be present in the red and white fired decorations, respectively. This is the first study, to our knowledge, that firmly identifies jacobsite in black decorations in Prehispanic archaeological ceramics.

In fragments recovered from one site, a carbon-based black pigment was identified while gypsum was observed in the recessed areas of decorative surface incisions. Gypsum, potassium nitrate and halite, most likely deposited during burial, were observed on the surface of some of the fragments analyzed. The results are discussed in the context of the technological processes involved and are compared to compositions previously reported for decorations in ceramic objects from NW Argentina.

1. Introduction

Archaeological assessments of ceramic production and consumption under Inca rule appear to be partially at odds with the insistence by historical narratives that the Inca exerted close control over their production enclaves, by overseeing the nature of the pottery and the distribution of the products. Over the years, numerous scholars have pointed out that Inca polychrome ceramics differ in style and manufacturing technique from one province to the other. This appears to be an inescapable consequence of the Inca reliance on local potters to produce state wares and on the spatially limited circulation of those pots [1,2].

In Northwestern (NW) Argentina, a region located in the Southern prolongation of the Andean Altiplano, that borders with Bolivia on the north and with Chile on the west, the Late Intermediate Period (LIP, ca. 900 AC–1430 AC) featured a marked population growth, an expanded farming through irrigation, a settlement diversification, and the formation of settlement hierarchies. The LIP Period ceased in the early 1400s when the Inca conquered NW Argentina, where a conscious manipulation of the landscape towards deliberate political ends occurred, resulting in a shift from local to imperial regional management strategies in the Late Period (LP). For example, in the Calchaquí and Yocavil Valleys, the Inca built a series of sites that included provincial centers, way stations, and local communities with state precincts, such as Guitian and Tolombón [3].

The surface decorations on four ceramic fragments excavated in two the sites in NW Argentina, Angastaco and Tolombón, were selected for the present study. Raman spectroscopy, Fourier transform infrared spectroscopy (FTIR), micro-X-ray diffraction (μXRD), and X-ray fluorescence (XRF) were combined to characterize the black, white and red surface decorations in these samples.

Angastaco, located in the confluence of the Angastaco and Calchaquí rivers, was a large and multi-functional archaeological site. Tolombón, a pre-Inca multi-component site located in the south of the Calchaquí river, had fortified, residential, and agricultural sectors which combined ceremonial and craft production, all joined by a major Inca road system [4]. Thorough compositional studies of artifacts from these sites would allow a better understanding of the materials and manufacturing processes used and of their possible chronological changes to ultimately compare them to artifacts excavated from related sites.

In previous analytical studies of surface decorations in Prehispanic ceramics from Northern Argentina, scanning electron microscopy-energy dispersive X-ray spectrometry (SEM-EDS), XRF, XRD, and FTIR were used to identify red, black and white pigments

* Corresponding author. Tel.: +1 212 650 2114; fax: +1 212 396 5060.
E-mail address: silvia.centeno@metmuseum.org (S.A. Centeno).

0924-2031/$ – see front matter © 2011 Elsevier B.V. All rights reserved.
doi:10.1016/j.vibspec.2011.11.004

(see, for example [5–9]). In the particular case of the black decorations in which Mn was the main component, tentative molecular compositions are reported in these publications based on elemental analyses by SEM/EDS. The exception is a study of a black decoration in a Portezuelo de Aguada style ceramic fragment by Cremonte et al. [8] in which $CaMnCO_3$ was identified by FTIR.

The complete and firm identification of Mn-containing compounds present in black ceramics decorations can be particularly challenging. Mn oxides are generally difficult to identify by Raman spectroscopy due to their sensitivity to laser-induced decomposition, as well as various other difficulties discussed by numerous authors [10–16]. Manganese oxides often have structures that are complex, sometimes involving solid solutions, or are present in mixtures with other compounds, iron oxides among them [14,16,17]. In some cases X-ray diffraction lines are broad, indistinct or absent [18] making their identification by this technique problematic. However, IR offers an advantage over XRD for the identification of tetravalent manganese oxides in disordered samples [18].

2. Experimental

2.1. Samples

Results obtained on four samples from two Inca archaeological sites located in the Calchaquí-Yocavil valleys in NW Argentina are presented as representative of a total of 15 fragments from these two sites that were made available for analysis.

Raman and XRF analyses were carried out *in situ*, non-invasively, while microsamples were removed for μXRD, and FTIR. Two ceramic fragments were selected among those excavated from residential and patio sectors in Tolombón, T2A6C4N8P [2011]/2 T2 and A6C6N7 [3536]/4, and two from residential rooms excavated in Angastaco, ATORS [739]/7 and ATOR1N1 [547]/11.

2.2. XRF

Qualitative and semi-quantitative X-ray fluorescence measurements were performed under a He atmosphere on different areas of the ceramic fragments, surface decorations and ceramic bodies, for equal live-times of 200 s at 40 kV and 600 μA, using a Bruker ARTAX 400 XRF spectrometer equipped with a Rh tube and a 650 μm collimator. A Si drift X-ray detector with a 10 mm^2 active area was used. The beam was focused on the different spots using the camera attached to the spectrometer.

2.3. FTIR

Fourier transform infrared spectroscopy measurements were carried out with a Bruker Vertex70® spectrometer coupled to a Hyperion® microscope. The samples were mounted between the windows of a diamond anvil cell and were observed in the transmission mode, with a spectral resolution of 4 cm^{-1}.

2.4. XRD

Micro X-ray diffraction patterns were measured using a Rigaku D/Max Rapid Diffractometer. Microscopic sample scrapings were mounted on glass fibers using Elmer's® glue. The instrumental parameters used were as follows: Cu Kα (λ = 1.542 Å) radiation (50 kV acceleration voltage and 40 mA current), chi (χ) fixed at 45°, omega (ω) fixed at 0°, phi (φ) spun from 60° to 120° at 1° s^{-1}, 0.8 mm collimator, and 10 min exposure times.

Open architecture X-ray diffraction measurements were carried out in selected samples, mainly to identify salt accretions visible on the surfaces of the fragments, using a Philips PW1835 open architecture design diffractometer with Cu Kα (λ = 1.542 Å) radiation (35 kV acceleration voltage, and 35 mA current). The fragments were placed in the instrument platform and the different areas of interest were analyzed *in situ* using a 10 mm × 2 mm mask.

Experimental diffraction patterns were matched with reference patterns (PDFs) in the ICDD (International Center for Diffraction Data) database using the Jade 8.0 (MDI Inc.) software in the case of the micro-diffraction measurements and the Jade 9.0 software for the open architecture measurements.

2.5. Raman microspectroscopy

Raman microspectroscopy analyses were carried out with a Renishaw System 1000 configured with a Leica DM LM microscope, notch filters, and a thermoelectrically cooled charged-coupled device (CCD) detector. A 785 nm laser line was used for excitation and was focused on the different areas of the ceramic fragments using the 50× objective lens of the microscope attached to the spectrometer, achieving a lateral resolution of ~2–3 μm. In order to avoid changes of the materials due to overheating, neutral density filters were used to set the laser power at the sample to values between 0.2 and 1.0 mW. A 1200 lines/mm grating was used and integration times were set between 10 and 300 s. The wavenumber stability and the accuracy were checked by recording the Raman spectrum of a silicon wafer (520 cm^{-1}).

Mn-containing black decorations in the ceramic fragments were analyzed using the minimal laser power available (0.2 mW), in order to reduce the chances of sample heating and consequent decomposition of sensitive Mn oxides.

3. Results and discussion

Representative samples were selected for analysis based on visual differences in their surface decorations to include black over red, black over white, black and white over a grey-brownish substrate, and red patterns over white. The decorations analyzed in the different fragments are shown in Fig. 1.

3.1. Black over red

The ATORS [739]/7 fragment has a black decoration applied over a red background (Fig. 1a). Raman analysis of the red background gave peaks characteristic of hematite (α-Fe_2O_3) at ca. 225, 245, 293, 410, 498, and 611 cm^{-1} [19] (Fig. 2, spectrum a). The presence of Al, Si, K, and Ti observed by XRF indicates that most likely the iron-containing compound was applied in clay form.

In the Raman spectrum recorded of the red decoration, the weak broad band present at ca. 660 cm^{-1} is characteristic magnetite Fe_3O_4 [19]. The presence of magnetite could be due to an incomplete phase transformation during firing, however, in an oxidizing atmosphere, this compound converts to maghemite (γ-Fe_2O_3) at the relatively low temperature of 200 °C and then to hematite at 400 °C [19,20]. Nonetheless, it should be pointed out that the activation energy for the transformation of maghemite into hematite depends on previous heat treatments and on the presence of other ions, such as aluminum [20].

XRF spectra generated for the black-on-red motif in ATORS [739]/7 showed that Mn and Fe are the most abundant elements, along with Cl. Cl was also detected in the red areas and it is likely due to salt accretions formed in the burial environment.

The μXRD pattern generated for this black decoration was an excellent match for the spinel jacobsite $MnFe_2O_4$ (PDF #00-010-0319) and hematite (PDF #98-000-0240) as the major phases, along with quartz (PDF #01-079-1910) (Fig. 3). Several peaks observed

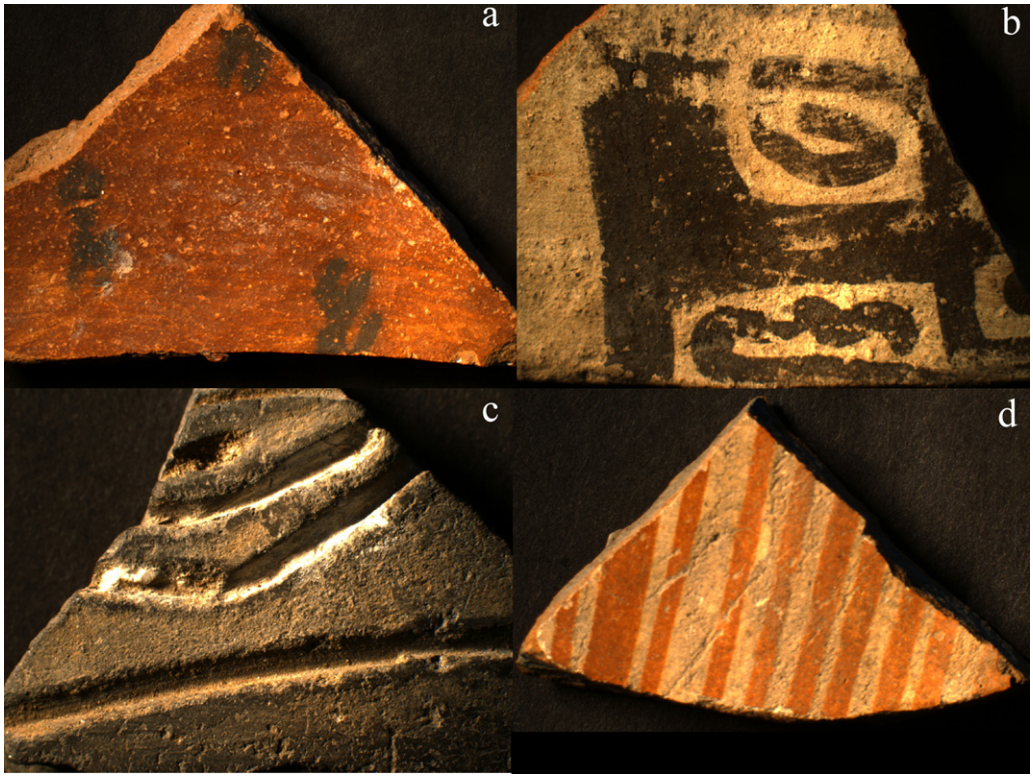

Fig. 1. Ceramic fragments with surface decorations analyzed: ATORS [739]/7 (a); T2A6C4N8P [2011]/2 (b); T2A6C6N7 [3536]/4 (c); and ATOR1N1 [547]/11 (d), respectively. The full widths of all photomicrographs are approximately between 3 and 4 cm.

in this pattern could not be matched to any phases in the ICDD database.

Raman spectra recorded in this black decoration showed a broad intense band at ca. 649 cm^{-1} and a weaker broad feature at ca. 448 cm^{-1} (Fig. 2, spectrum b), confirming the presence of jacobsite as detected by μXRD. An intense broad Raman band has been reported for jacobsite at ca. 640 cm^{-1}, along with two weak broad bands at ca. 339 and 456 cm^{-1} [17]. The peaks at ca. 225, 293, 410, 498, and 611 cm^{-1} in the spectrum b in Fig. 2 are due to hematite present in the red background.

To avoid laser-induced decomposition a 0.2 mW laser power was used to record the Raman spectra in all the black decorations. No changes in the spectra were observed when a water droplet was applied before the acquisition, as recommended by several authors [10,13,15].

It has been stated that pyrolusite, MnO_2, transforms into bixbyite, α-Mn_2O_3 at 500 °C, that the latter is stable until approximately 800 °C [11], and that at higher temperatures (900–1000 °C) bixbyite reacts with hematite to form jacobsite [21]. It is not

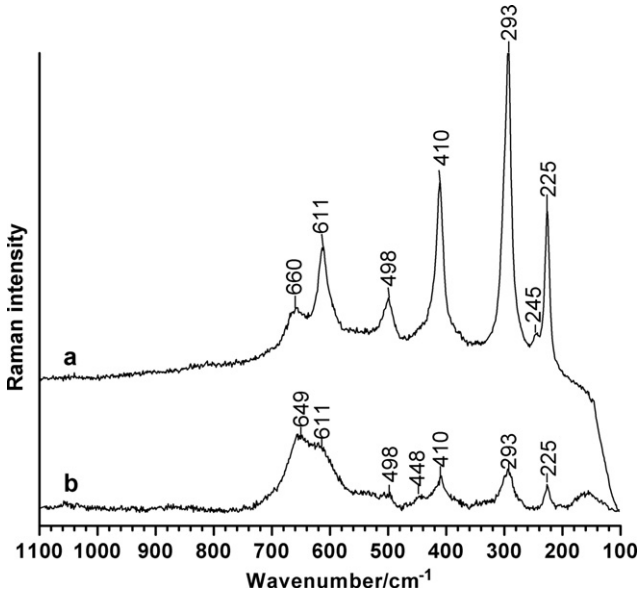

Fig. 2. Sample ATORS [739]/7. Raman spectra of recorded in the red (a) and in the black areas of the decoration (b), respectively. λ_0 = 785 nm.

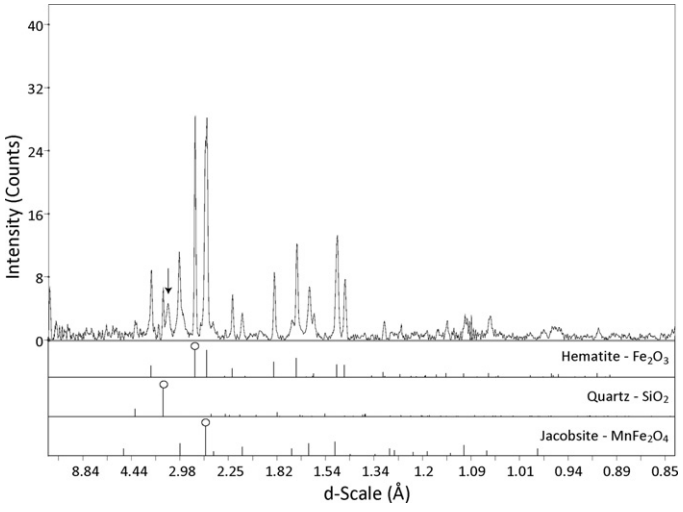

Fig. 3. Micro-XRD pattern recorded in a sample scraping on the black decoration in ATORS [739]/7, showing the presence of jacobsite, $MnFe_2O_4$, hematite and quartz. Unassigned peaks are indicated by an arrow.

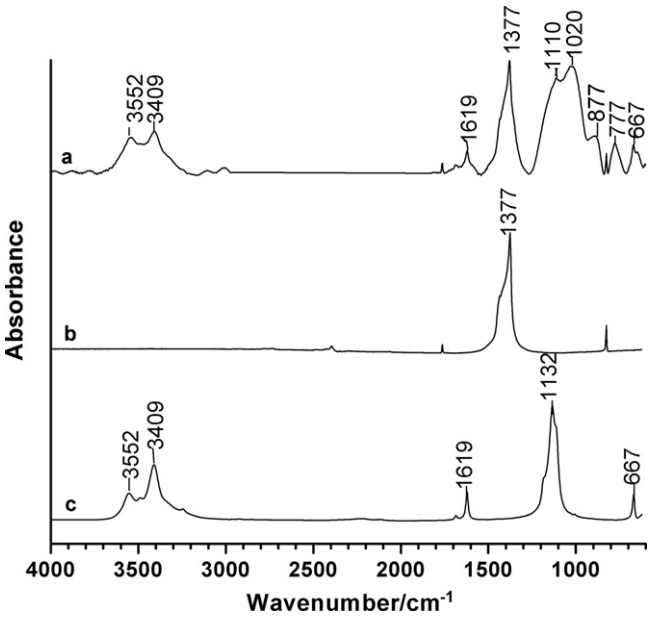

Fig. 4. FTIR spectrum recorded in the white background of T2A6C4N8P [2011]/2 (a), shown along with reference spectra for KNO_3 (b) and gypsum, $CaSO_4{\cdot}2H_2O$ (c).

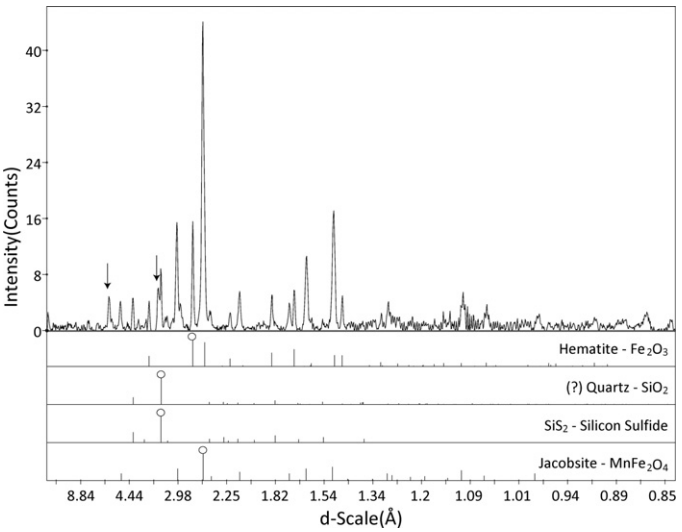

Fig. 5. XRD pattern of the black decoration in the fragment T2A6C4N8P [2011]/2. Unidentified peaks are indicated by an arrow.

possible, in this case, to estimate the firing temperature without information about the original Mn-containing ores used.

3.2. Black over white

T2A6C4N8P [2011]/2 has a black decoration applied over a creamy white background (Fig. 1b). XRF analysis showed that the white areas contain relatively large amounts of Ca and Cl compared to the ceramic substrate, along with Al, Si, P, S, K, Ti, Mn and Fe. All these elements, except for P, were also found to be present in the ceramic substrate.

The FTIR spectrum acquired in a microsample removed from the white decoration is shown in Fig. 4 (top spectrum). In this spectrum, the intense broad bands present at ca. 1020 and 1110 cm^{-1} and the peak at ca. 777 cm^{-1} can be assigned to Si–O–Si and Si–O–Al stretch frequencies in silicates [22]. In this spectrum, gypsum ($CaSO_4{\cdot}2H_2O$) and KNO_3 are also identified. Reference spectra for these two compounds are included in Fig. 4 for comparison. The bands at ca. 3409 and 3552 cm^{-1} in the top FTIR spectrum in this figure are due to the υ_{H_2O} vibrations in gypsum. Layer silicates have hydroxyl stretching bands between 3400 and 3750 cm^{-1} that shift when the material is heated and finally disappear at ca. 600 °C [22–24]. Although the presence or absence of these features can be used to estimate the firing temperature of clay materials, the bands attributed to gypsum in this sample overlap the range where these silicate hydroxyl bands are expected.

In agreement with the FTIR results, Raman spectra recorded in the white decoration in this fragment showed weak peaks at ca. 460 cm^{-1} and at ca. 1040 cm^{-1}, characteristic of Si–O bend and stretch modes of amorphous silicates (spectrum not shown) [25].

Mn and Fe were the major components observed by XRF in the black decoration. Raman spectra generated in this black decoration using a very low laser power, 0.2 mW, show a broad band at ca. 640 cm^{-1} that can be attributed to jacobsite (Fig. 6, spectrum a) [17]. A second broad band observed in this spectrum at ca. 691 cm^{-1} is also within the range expected for the Mn–O stretching vibrations, between 600 and 750 cm^{-1} [11]. However, more precise assignments around this frequency are not without controversy. Biciuman et al. report a feature at 680 cm^{-1} as characteristic of α-Mn_2O_3 bixbyite, and assign a peak in the range of 650–640 cm^{-1} to Mn_3O_4 resulting from the degradation of Mn_2O_3 during the analysis [12]. Conversely, the position of the characteristic band of α-Mn_2O_3 is reported at 592 cm^{-1} by Julien et al. [11].

μXRD analysis performed on a microscopic sample removed from the black decoration confirmed the presence of jacobsite $MnFe_2O_4$ (PDF #00-010-0319) as a major phase, with minor phases of hematite (PDF #98-000-0240), silicon sulfide (PDF #00-047-1376) and/or quartz (PDF #01-079-1910) (Fig. 5). As in the case of the black decoration in ATORS [739]/7, several peaks observed in this pattern could not be matched to any phases in the ICDD database.

Open architecture XRD analyses were performed on the surface of the fragment where white salt deposits are visible. In both the white and black areas, halite (NaCl, PDF #04-006-5374) and gypsum ($CaSO_4{\cdot}2H_2O$, PDF #04-008-9805) were identified, consistent with the presence of Ca, S and Cl observed by XRF. These two salts, as well as the KNO_3 identified by FTIR, most likely originated in the burial environment.

3.3. Black and white over a brown substrate

The decoration on the T2A6C6N7 [3536]/4 fragment consists of a black motif applied over a brown ceramic surface. Incised lines on the ceramic body notably contain a white material filling the recessed areas (Fig. 1c). This white pigment was identified as gypsum by its characteristic Raman bands at ca. 1135, 1008, 671, 619, 492 and 412 cm^{-1} (Fig. 6, spectrum b) [26]. FTIR analysis performed on a microscopic sample of the white pigment confirmed the presence of gypsum. Calcium and sulfates have been previously reported in a technical study of similar decorations in *Famabalasto Negro Grabado* style ceramics [27]. No organic compounds that could have been used as binding media to keep the pigment particles together and attached to the ceramic surface, were detected by FTIR (Fig. 7, spectrum a). The apparent absence of a binder in similar decorations in *Famabalasto Negro Grabado* ceramics has been noted before [27,28]. It is possible that the concentration of the organic material in the samples analyzed for the present study is below the detection limit of FTIR. Although additional analysis by gas chromatography–mass spectrometry (GC–MS) could shed light on the presence or absence of a binder, the sample size required made the use of this technique unsuitable for this study.

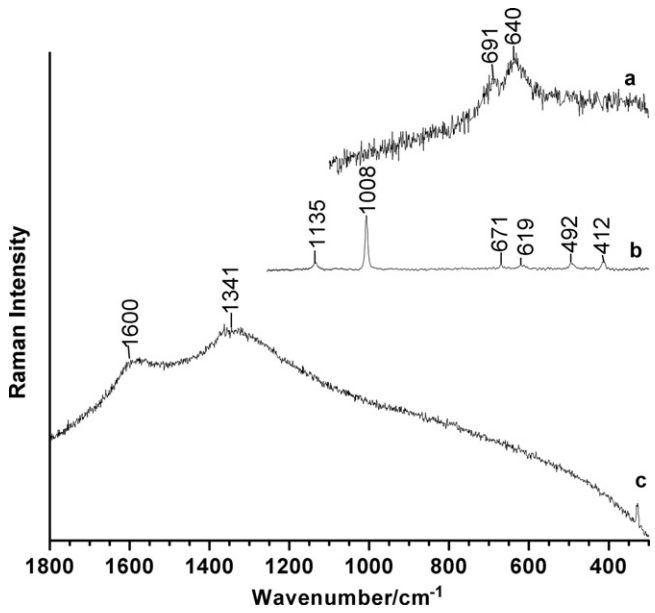

Fig. 6. Raman spectra recorded in the black dark decoration in T2A6C4N8P [2011]/2 (a), in the white pigment in the incisions in T2A6C6N7 [3536]/4 (b), and in the black paint decoration in T2A6C6N7 [3536]/4 (c), respectively. λ_0 = 785 nm.

Raman spectra generated in the black decoration exhibited two broad bands at ca.1590 and 1340 cm^{-1}, which are characteristic of a carbon-based black pigment, such as charcoal or lamp black (Fig. 6, spectrum c). Reference samples of charred bone give similar features with an additional band at ~961 cm^{-1} resulting from the PO_4^{3-} in the bone hydroxyapatite [10,26,29], however this band is not always visible in samples from real artifacts. The phosphate characteristic band was not observed in the Raman spectrum recorded, nor was P detected by XRF.

3.4. Red over white

The sample ATOR1N1 [547]/11 has a decoration that consists of red stripes applied over a white background (Fig. 1d). The white background was found to contain Al, Si, P, S, Cl, K, Ca, Ti, Mn, and Fe by XRF. All these elements were also observed in the ceramic substrate, where the proportions of Cl, Ti, and Fe were found to be relatively higher, and those of Ca and S were found to be lower compared to the white decoration. Al, Si, K, and Ti indicate the presence of a clay. An FTIR spectrum representative of those recorded in the white areas is shown in Fig. 7, spectrum b. In this spectrum, the broad and weak hydroxyl stretch band in the range of 3200–3600 cm^{-1} is indicative of a clay material that has been fired at ca. 600 °C or higher temperatures [22–24]. The dehydroxylation of the silicate material in this white decoration was accompanied by amorphization as indicated by the broad band at ca. 1060 cm^{-1} with a shoulder at ca. 1190 cm^{-1}, characteristic of Si–O modes in a disordered structure [23].

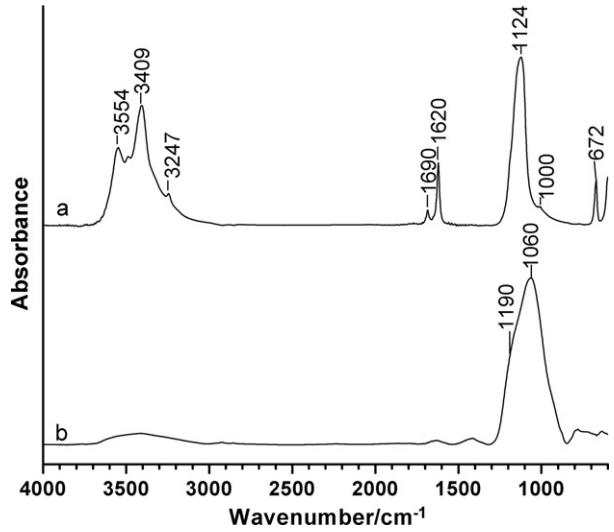

Fig. 7. FTIR spectra recorded in the white pigment present in the incisions in T2A6C6N7 [3536]/4 (a), and in the white layer in ATOR1N1 [547]/11 (b), respectively.

XRF elemental analysis of the red decoration showed that Fe is the main component. Raman spectra recorded in the red stripes showed bands at ca. 225, 294, 411, and 609 cm^{-1} due to hematite, indicative of an oxidizing atmosphere during firing, and also a band at 461 cm^{-1} pointing to the presence of quartz (spectrum not shown) [30].

4. Conclusions

The decorations in pottery fragments excavated in Angastaco and Tolombón, two archaeological sites located in Northwestern Argentina and dating to the Inca period, were investigated with a multitechnique approach that included Raman spectroscopy, FTIR, μXRD and XRF. This combination of microanalytical techniques proved indispensable to fully identify the components in the decorations.

In the all red decorations, hematite was identified by Raman, indicating oxidizing conditions during firing. The combination of μXRD with Raman spectroscopy allowed to unambiguously determine the presence of the spinel jacobsite, $MnFe_2O_4$, in the fired black decorations in two fragments, and therefore to overcome the difficulties normally encountered in the analysis of black and brown manganese-containing materials by vibrational techniques only.

The composition and approximate firing temperature of the white decoration in one of the fragments could be determined from the analysis of the FTIR spectra, complemented by XRF. In this case, the white paint was found to contain mainly a clay fired at a temperature no lower than 600 °C. In the white decoration on a second sample, the presence of bands due to gypsum in the FTIR spectrum hindered the identification of the characteristic silicate hydroxyl bands that would allow an estimation of firing temperature. For this decoration, the presence of an amorphous silicate could be determined from the analysis of its Raman spectrum.

Similar materials have been previously reported in red and white ceramic decorations in artifacts from other sites in NW Argentina, however, this is the first study, to our knowledge, that identifies jacobsite in the black decorations.

In addition to the fired red, black and white motifs, incised lines containing gypsum were observed in one fragment from Tolombón. These results are consistent with those reported by other authors in studies of similar decorations in *Famabalasto Negro Grabado* ceramics. Painted motifs containing a carbon-based black pigment were observed in the same fragment. These pigments must have been applied with an organic binder, but this material was found to be below the detection limit of FTIR.

Acknowledgments

The authors are indebted to Tony Frantz, Research Scientist at The Metropolitan Museum of Art, for generously sharing his expertise in XRD.

References

[1] V. Williams, T.N. D'Altroy, in: I. Farrington, R. Raffino (Eds.), Tawantisuyu, Australian National University, 1998, pp. 170–178.

[2] T.N. D'Altroy, A.M. Lorandi, V.I. Williams, M. Calderari, C. Hastorf, E. DeMarrais, M.B. Hagstrum, J. Field Archaeol. 27 (2000) 1–26.
[3] V. Williams, in: P. González Carvajal, T.L. Bray (Eds.), Lenguajes Visuales de los Incas, Archaeopress, Oxford, 2008, pp. 47–70.
[4] V. Williams, Anales NE Inst. Iberoamericano 6 (2003) 163–210.
[5] G.A. De La Fuente, N. Kristcautzky, G. Toselli, A. Riveros, Estud. Atacameños 30 (2005) 61–78.
[6] G.A. De La Fuente, N. Kristcautzky, G. Toselli, in: M.B. Cremonte, N. Ratto (Eds.), Cerámicas Arqueológicas. Perspectivas Arqueomètricas para su Análsis e Interpretación, Universidad Nacional de Jujuy, Jujuy, 2007, pp. 39–47.
[7] M.d.P. Babot, M.C. Apella, in: M.B. Cremonte, N. Ratto (Eds.), Cerámicas Arqueológicas. Perspectivas Arqueomètricas para su Análsis e Interpretación, Universidad Nacional de Jujuy, Jujuy, 2007, pp. 13–26.
[8] M.B. Cremonte, M. Baldini, L.I. Botto, Intersec. Antropol. 4 (2003) 3–16.
[9] M.A. Lopez, in: M.B. Cremonte, N. Ratto (Eds.), Cerámicas Arqueológicas. Perspectivas Arqueomètricas para su Análsis e Interpretación, Universidad Nacional de Jujuy, Jujuy, 2007, pp. 169–185.
[10] G.D. Smith, R.J.H. Clark, J. Archaeol. Sci. 31 (2004) 1137–1160.
[11] C.M. Julien, M. Massot, C. Poinsignon, Spectrochim. Acta A 60 (2004) 689–700.
[12] F. Buciuman, F. Patcas, R. Cracium, D.R.T. Zahn, Phys. Chem. Chem. Phys. 1 (1999) 185–190.
[13] M.-C. Bernard, A. Hugot-Le Goff, B.V. Thi, S.C. de Torresi, J. Electrochem. Soc. 140 (1993) 3065–3070.
[14] D.C. Smith, M. Bouchard, M. Lorblanchet, J. Raman Spectrosc. 30 (1999) 347–354.
[15] F. Ospitali, D.C. Smith, M. Lorblanchet, J. Raman Spectrosc. 37 (2006) 1063–1071.
[16] M.C. Caggiani, P. Colomban, J. Raman Spectrosc. 42 (2011) 839–843.
[17] R.J.H. Clark, Q. Wang, A. Correia, J. Archaeol. Sci. 34 (2007) 1787–1793.
[18] R.M. Potter, G.R. Rossman, Am. Miner. 64 (1979) 1199–1218.
[19] D.L.A. deFaria, S.V. Silva, M.T. de Oliveira, J. Raman Spectrosc. 28 (1997) 873–878.
[20] F.E. De Boer, P.W. Selwood, J. Am. Chem. Soc. 76 (1954) 3365–3367.
[21] G.E. De Benedetto, S. Nicoli, A. Pennetta, D. Rizzo, L. Sabbatini, A. Mangone, J. Raman Spectrosc. 42 (2011) 1317–1323.
[22] V.C. Farmer, The Infrared Spectra of Minerals, Mineralogical Society, London, 1974.
[23] M.R. Derrick, D. Stulik, J.M. Laundry, Infrared Spectroscopy in Conservation Science. Scientific Tools for Conservation, The Getty Conservation Institute, Los Angeles, 1999.
[24] A. Mangone, L.C. Giannossa, G. Colafemmina, R. Laviano, A. Traini, Microchem. J. 92 (2009) 97–102.
[25] P. Colomban, Treppoz, J. Raman Spectrosc. 32 (2001) 93–102.
[26] L. Burgio, R.J.H. Clark, Spectrochim. Acta A 57 (2001) 1491–1521.
[27] V. Palamarczuk, Un estilo y su época. El caso de la cerámica Famabalasto Negro Grabado del Noroeste Argentino, Facultad de Filosofia y Letras, University of Buenos Aires, Buenos Aires, 2009.
[28] E.M. Cigliano, Rev. Museo Plata (Nueva Serie) 24 (1958) 29–122.
[29] I.M. Bell, R.J.H. Clark, P.J. Gibbs, Spectrochim. Acta A 53 (1997) 2159–2179.
[30] R.K. Sato, P.F. McMillan, J. Phys. Chem. 91 (1987) 3494–3498.